

Review

# A Critical Review of Mg-Based Hydrogen Storage Materials Processed by Equal Channel Angular Pressing

Lisha Wang <sup>1</sup>, Jinghua Jiang <sup>1,\*</sup>, Aibin Ma <sup>1,2</sup>, Yuhua Li <sup>1,2</sup> and Dan Song <sup>1</sup>

<sup>1</sup> College of Mechanics and Materials, Hohai University, Nanjing 211100, China; lisawangzf@163.com (L.W.); aibin-ma@hhu.edu.cn (A.M.); sduhua@126.com (Y.L.); songdancharls@hhu.edu.cn (D.S.)

<sup>2</sup> Suqian Institute, Hohai University, Suqian 223800, China

\* Correspondence: jinghua-jiang@hhu.edu.cn; Tel.: +86-25-8378-7239; Fax: +86-25-8378-6046

Received: 16 July 2017; Accepted: 18 August 2017; Published: 23 August 2017

**Abstract:** As a kind of cost-efficient hydrogen storage materials with high hydrogen capacity and light weight, Mg-based alloys have attracted much attention. This review introduces an effective technique in producing bulk ultrafine-grained (UFG) Mg alloys and promoting its hydrogen storage property, namely, equal-channel angular pressing (ECAP). This paper briefly describes the technical principle of ECAP and reviews the research progress on hydrogen storage properties of ECAP-processed Mg alloys. Special attention is given to their hydrogen storage behaviors including hydrogen storage dynamics, capacity, and cycling stability. Finally, it analyzes the factors that affect the hydrogen storage properties of ECAP-processed Mg alloys, such as the grain sizes, lattice defects, catalysts, and textures introduced by ECAP process.

**Keywords:** Mg alloy; hydrogen storage behavior; equal-channel angular pressing (ECAP)

## 1. Introduction

The US Department of Energy (DOE) has foretold a 37% increase in the world's energy demand by 2035, compared with that in 2008 [1,2]. Hydrogen fuel, a new kind of renewable and clean energy, has been considered as a promising candidate for an environmentally friendly source of alternative energy to the conventional fossil fuels in meeting the world's demand [3–5]. Technical issues, for instance hydrogen storage, must be overcome before its utilization in large-scale applications. For many years, metal hydride has attracted attention worldwide for its safe, cost-effective properties compared with other storage options such as high pressure gas tanks and cryogenic liquid, and it has already become a hot topic in the field of hydrogen storage. Numerous investigations have focused on Mg and its alloys, primarily due to their high hydrogen storage capacity, relatively low cost, and large abundance in the Earth's crust [4,5].

Hydrogen can be stored in Mg in the form of Mg-based metal hydrides during the process of dissociative chemisorption. Mg-based metal hydride can be generated by Mg and H<sub>2</sub> at a temperature of 300–400 °C and a hydrogen pressure of 2.4–40 MPa [6]. The formation equation can be described as:



MgH<sub>2</sub> has the highest hydrogen storage densities, up to 7.6 wt % [7], compared with other hydrides applicable for hydrogen storage. The enthalpy of MgH<sub>2</sub> formation,  $\Delta H = -74.7$  kJ/mol, which makes the equilibrium hydrogen evolution temperature at a standard atmospheric pressure, is as high as 289 °C. Concerning its mechanism of operation, there are four steps required for hydrogen to be stored in Mg alloys: (1) H<sub>2</sub> dissociates on the surface of the Mg alloy. In this step, surface properties

such as morphology and surface structures as well as the purity of the Mg alloy are among the factors influencing H<sub>2</sub> dissociation; (2) Diffusion of the dissociated H atoms in the Mg alloy. In this stage, the microstructures of Mg including the grain size and grain boundaries represent the most important issues for the diffusion of H atoms inside the metal; (3) The formation of the hydrogen-containing solid solution inside Mg. In this stage, microstructure defects such as dislocations and vacancies are necessary aspects to be considered; (4) Phase transformation takes place between H atoms and Mg to form MgH<sub>2</sub>. In this stage, catalysts play an important role in the transformation.

As mentioned above, the slow hydrogen absorption and desorption kinetic and high working temperatures above 250 °C are the most obvious barriers to the development of Mg as a hydrogen storage carrier. Widespread research has been conducted over the past couple of decades to solve those problems, with significant advancements achieved through mainly focused on improving the H<sub>2</sub> dissociation ability as well as its diffusion inside the Mg matrix. One of the most effective methods is to reduce the Mg grain size to the nanoscale. Equal-channel angular pressing (ECAP), one of the severe plastic deformation (SPD) methods producing submicrometer and nanoscale grains with high angle grain boundaries, has been used to refine bulk coarse-grained metals and alloys to grain sizes ranging from a few tens to a few hundreds of nanometers without changing the bulk dimensions. ECAP could introduce an ultra-fine grained (UFG) structure with excellent mechanical properties, as well as unique physical and chemical performances. Intensive research had been carried out in the application of UFG alloy processed by ECAP, for example, in fabricating various micro-parts working in micro-electro-mechanical systems [8] and in making biodegradable stents in the biomedical field [9]. ECAP also can be used in improving the hydrogen storage property of Mg-based hydrogen storage materials. The ECAP process creates defects such as vacancies and dislocations which produce a positive effect on the diffusion kinetics. Investigations suggested that there was an improvement in the diffusion and H<sub>2</sub> storage capacity in Mg alloys after being processed by SPD due to the presence of excess vacancies.

In this review, we briefly introduce ECAP as an effective process technique in producing bulk UFG Mg alloy. We mention the hydrogen storage behaviors of ECAP-processed UFG Mg alloys, such as hydrogen storage dynamics, capacity, and cycling stability. A brief review of state-of-the art is reported on the hydrogen storage properties of ECAP-processed Mg alloys. This work will serve to enrich the preparation of solid-state hydrogen storage systems in order to realize the long-term application of Mg-based hydrogen storage alloys.

## 2. ECAP Technology

Mg alloys have been intensively studied for possible applications as a kind of hydrogen storage material due to their high hydrogen storage capacity, better cycling stability, and relatively low cost. Nevertheless, the critical assessment of an Mg-H system based on thermodynamic modeling of different stable phases indicated that the hydrogen desorption temperature under 1 bar was above 423 K. Besides, the hydrogen desorption rate at 423 K is quite slow. Those factors could hinder the practical application of magnesium-based hydrogen storage materials [10]. The recent progress in the field of nanocrystalline material has given hope for the improvement of the hydrogen storage properties of Mg, as well as promoted the application of magnesium alloys in hydrogen storage materials [11]. Nanocrystalline solids can provide a high density of lattice defects. A great amount of atoms in nanocrystalline materials may be located in the defect cores with distorted coordination [11], like large angle grain boundaries. Also, the parameters of the interaction between those atoms with hydrogen must be fairly different from that found in perfect solids. It has already been proved experimentally that such nanostructure hydrides of Mg offer better kinetics than their coarse-grained counterparts. Moreover, grain boundaries also provide easy paths for the diffusion of H atoms into the bulk. A high density of defects inside the bulk together with its microstructure can effectively affect the hydrogen storage property during the absorption and desorption processes of nanostructure Mg-based hydrogen storage materials.

ECAP is an attractive technology in producing nanocrystalline materials, and can offer factors that could influence the final microstructure. ECAP was first introduced by Segal et al. [12]. A large number of reports have described the process of metal flow during ECAP.

As shown in Figure 1a, the die contains an internal channel and an external channel.  $\Phi$  and  $\Psi$  represent the channel angle and the curvature angle, respectively. Samples made in cuboid shapes are pushed through the die by a plunger. To make it simple,  $\Phi$  in Figure 1a is about  $90^\circ$ . Figure 1b illustrates the theoretical shear plane [13] existing in the die when the samples go through the two channels. When passing through the die, samples are exposed to the simple shear strain which cause the imposed deformation on them without any changes in the cross-sectional dimensions. With the same cross-section, samples can be processed repetitively to attain a high strain. Severe deformation, appearing during the process, will lead to grain refinement, in some circumstances to the nanoscale.

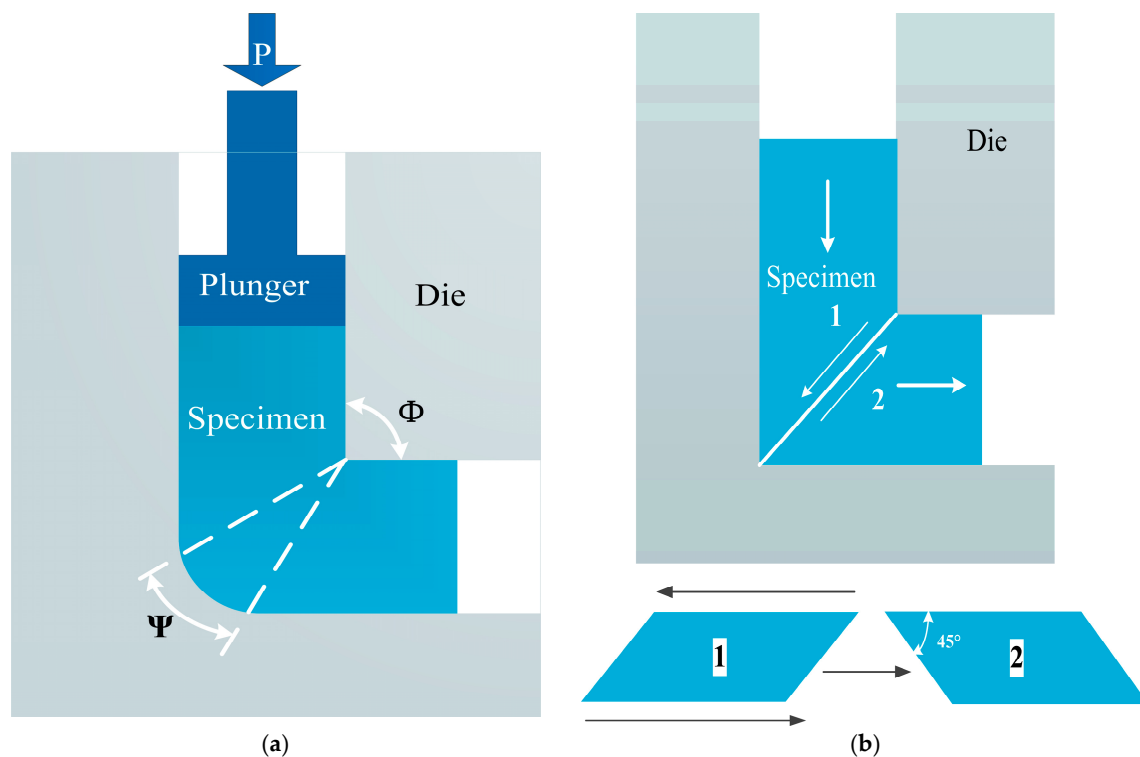


**Figure 1.** (a) The schematic illustration of a typical ECAP (equal channel angular pressing) facility; (b) The principle of ECAP showing the shearing plane existing in the die.

Samples passed through the die once indicates one pass processed by ECAP. ECAP passes play a key role in the deformation process, the equivalent strain after  $N$  passes, can be expressed in a general equation [14]:

$$\varepsilon_N = \frac{N}{\sqrt{3}} \left[ 2 \cot \left( \frac{\Phi}{2} + \frac{\Psi}{2} \right) + \Psi \operatorname{cosec} \left( \frac{\Phi}{2} - \frac{\Psi}{2} \right) \right] \quad (2)$$

$\Phi$  and  $\Psi$  represent the angles in Figure 1a. As the number of passes increases, samples are exposed to an increased strain which could lead to a further grain refinement. Between passes, the billet can be rotated around its longitudinal axis. As illustrated in Figure 2, there are three main pressing routes in the use of ECAP: In route A, samples can be pressed repetitively with no rotation. In route B, samples are rotated by  $90^\circ$  in the same direction between the passes. In route C, the samples are rotated by  $180^\circ$  between the passes [15].

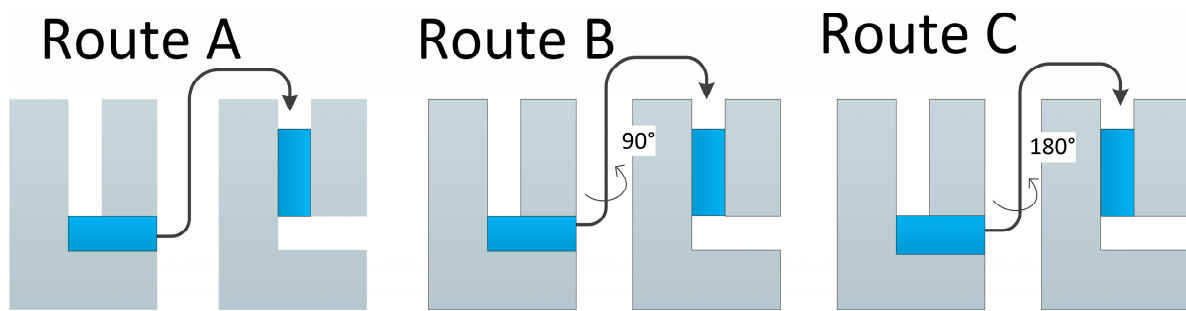


Figure 2. Characteristics of most important ECAP processing routes.

The repetitive passes, together with the combination of different routes, strongly determines the final microstructure of the material [16,17]. As shown in Figure 3, after 12 passes through the ECAP process by route B, the coarse  $\beta$ -phase was refined to about  $10\ \mu\text{m}$  and then homogeneously distributed in the  $\alpha$ -phase Mg matrix, shown in the work by Song et al. [18]. Except for the UFG metallic materials, ECAP can also provide a higher density of lattice defects such as vacancies and dislocations.

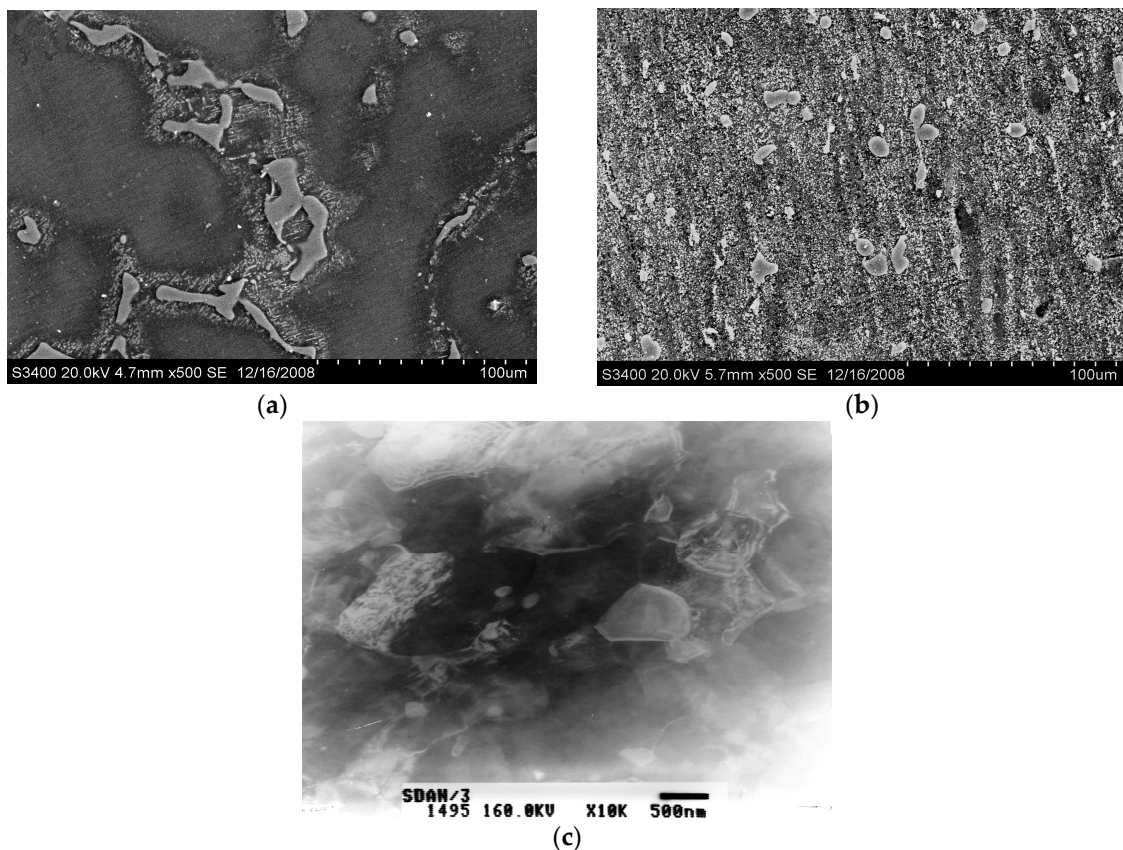


Figure 3. UFG (ultrafine-grained) grains of  $\alpha$ -Mg phase and the highly refined secondary phase. (a) SEM image of as-cast AZ91; (b) SEM image of AZ91 after 12 ECAP passes; (c) TEM images of AZ91 after 12 ECAP passes. Reproduced with permission from [18], Elsevier, 2011.

### 3. Effect of ECAP on the Hydrogen Storage Behavior of Mg-Based Metal Hydrides

#### 3.1. Dynamics

Hydrogen storage dynamics is a basic issue in hydrogen storage property. It can be defined as the speed of hydrogen absorption/desorption of a material. Activation or incubation time,

the time required for the material starting to absorb hydrogen, is another factor to testify hydrogen storage dynamics.

According to Skripnyuk [11], the first scholar to have investigated the effect of ECAP on the hydrogen storage properties of Mg alloy hydrides, commercial Mg alloy ZK60 showed a higher hydrogen storage property in both hydrogen capacity and the pressure hysteresis after eight passes of ECAP compared with its as-cast counterparts.

His later work [19] was focused on the effect of ECAP on the hydrogen storage properties of a eutectic Mg-Ni alloy. The eutectic alloy  $Mg_{89}Ni_{11}$  was processed by ECAP, with  $\Psi = 90^\circ$  and  $\Psi = 0^\circ$  through route B for 10 passes. The process was started at the temperature of 573 K during the first pass, and the temperature decreased to 513 K and 503 K during the ninth and 10th passes. Samples were hydrogenated at 573 K and a hydrogen pressure of 25 atm, and then processed by five desorption/absorption cycles. The kinetics of hydrogen desorption from ECAP-processed and as-cast alloys at 573 K shown in Figure 4 indicates that samples processed by 10 ECAP passes took less time to desorb up to 6 wt % of hydrogen. Herein, it took 10 min for as-cast samples but only 6 min for ECAP-processed samples. Besides, the Van't Hoff diagrams for the desorption processes of ECAP-processed Mg and as-cast Mg hydrides showed that the entropy of  $MgH_2$  for the ECAP-processed Mg alloy samples was higher than that of their as-cast counterparts. A shorter incubation time was also found in the research by Asselli et al. for ZK60 hydrogen storage material after six ECAP passes [20].

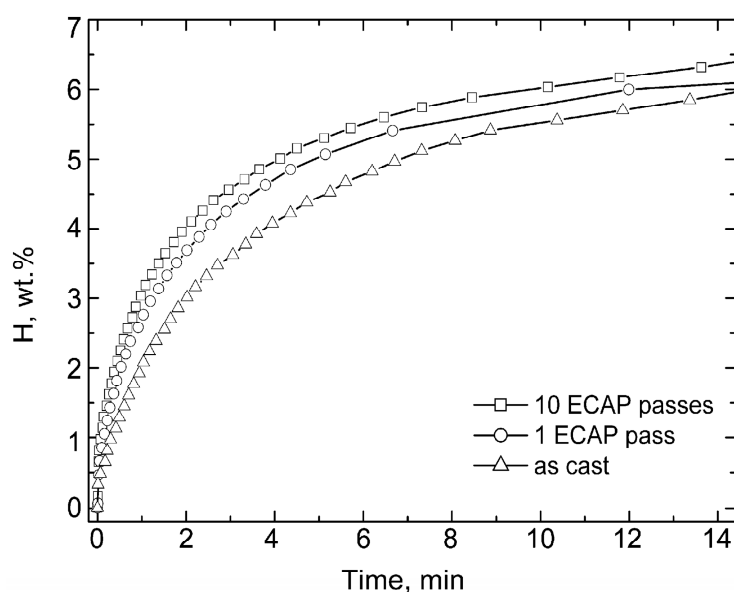


**Figure 4.** Kinetics of hydrogen desorption at 573 K in as-cast and ECAP-processed samples Reproduced with permission from [19], Elsevier, 2007.

### 3.2. Capacity

To investigate the effect of ECAP on Mg-based hydrogen storage material systematically, hydrogen storage capacity is important. Hydrogen storage capacity gives a clear description of how much hydrogen will be absorbed/released for a hydrogen storage material.

As shown in Figure 4, after 10 ECAP passes through route B, with the hydrogenated temperature at 573 K and a hydrogen pressure of 25 atm, the gravimetric hydrogen storage capacity of eutectic alloy  $Mg_{89}Ni_{11}$  can be as high as 6 wt % [19].

However, other research showed that processing ZK60 only by ECAP can barely improve the hydrogen storage capacity [21]. In the research of severely deformed ZK60 + 2.5% Mn alloy for hydrogen storage produced by two different processing routes, samples with the composition

Mg<sub>5</sub>Zn<sub>1</sub>Zr<sub>2.5</sub>Mm were processed by both ECAP and a combination of ECAP and Cold Rolling (CR). The absorption measurement was conducted at 623 K and a hydrogen pressure of 20 bar (2 MPa). The result was quite interesting, showing that the samples after four ECAP passes provided relatively fast activation but a fairly small storage capacity about 2.5 wt % of H<sub>2</sub> [21]. When ECAP was combined with CR, the hydrogen capacity could be highly promoted, which reached about 4 wt % of H<sub>2</sub> [21]. Analogical results can be found in other studies, which suggests that the ECAP followed by CR could be a useful method in improving bulk magnesium hydrogen storage material. From the microstructure point of view, the combination of ECAP and CR highly contributed to the creation of a strong (002) texture [15]; evidence showed that when there appears a (002) texture in the matrix, the kinetics of Mg hydrogen storage property could be highly enhanced [22]. Furthermore, the combination of ECAP and CR could also achieve the goal of breaking the intermetallic phases as well as introducing microstructural defects, which are the factors responsible for the improvement in hydrogen storage properties of Mg-based hydrogen storage materials. Those factors will be precisely described later in Section 4.

### 3.3. Cycling Stability

During the processes of hydrogen absorption and desorption, the material will lose its reversible hydrogen storage capacity. The ability of the material to maintain its reversible hydrogen storage capacity is known as long-term cycling stability or cyclic stability [23]. Long-term cycling stability is a classic feature in determining hydrogen storage property.

When considering cycling stability, Krystian [24] carried out a long-term test of 1000 charging and discharging experiments. ZK60 Mg alloy was refined by ECAP using route B for four passes at a suitable temperature range from 383 K to 573 K. Hydrogenation experiments were carried out under a constant temperature between 473 K and 623 K with a pressure of hydrogen of about 1.5 MPa and 0–0.1 MPa. He found that the hydrogen capacity and kinetics of commercial ZK60 Mg alloy were both enhanced after ECAP processing. Except for 75% of the theoretical maximum storage capacity that had been reached within 1 h, the corresponding discharging time was reduced from 15 min to approximately 5 min. As shown in Figure 5, the result also presented an increase in the kinetics for the first 50 cycles, after which it increased slightly for the next 150 cycles, and remained at that level up to at least 1000 cycles [24].

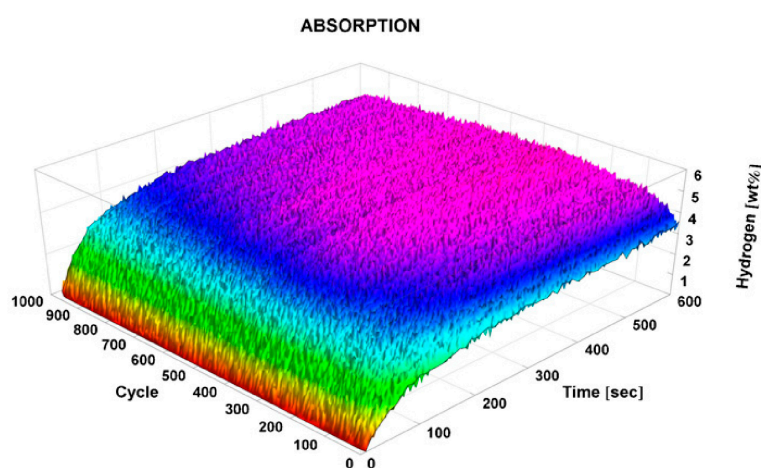


**Figure 5.** Color-coded 3D diagrams showing the storage capacity and kinetics of hydrogen at the absorption of ZK60 at 623 K against cycle number and time. Reproduced with permission from [24], Elsevier, 2011.

ZK60 processed by ECAP showed a better kinetics and high stability compared with that processed by other techniques like HEBM (high energy ball milling), doped Mg, HPT (high pressure torsion), and

CR (cold rolling), with respect to long-term investigations. The doped Mg alloys presented a decrease in storage capacity over the first 25 cycles [25]. Samples processed by HEBM performed better but still gave a considerable decrease in hydrogen storage capacity after just 60 cycles [26,27]. For HPT (high pressure torsion) processed samples, the cycling stability was maintained for at least 200 cycles, but was still far less than that processed by ECAP. Lastly, CR MgH<sub>2</sub> showed a lower dynamic performance than both ECAP- and HEBM-processed ZK60 in the first few cycles [28].

#### 4. Analysis of the Factors Affecting Hydrogen Storage Properties

##### 4.1. Grain Size and Crystallographic Defects

ECAP is a profitable technique to provide UFG metallic materials with a high density of lattice defects. Grain size and crystallographic defects such as vacancies and dislocations are considered as vital aspects that affect the hydrogen storage behavior of metal hydrides.

It had been proved that by reducing the grain size from 2600 nm to 300 nm, the kinetics become almost twice as fast [24]. The exact mechanism for grain size that affects Mg hydride's hydrogen storage property still remains unsolved. Yet, it is widely recognized that the finer grain size, the larger the surface area is, hence the easier it is for dissociated H atoms to diffuse into the Mg matrix.

As for Mg-H system, H atoms are trapped by vacancies when they enter interstitial sites of the Mg lattice; for each vacancy, it can capture up to six H atoms with large binding energy. According to Sato et al. [29], internal strain is a leading cause of the formation of vacancies. During ECAP processes, the strain occurring on Mg alloys is large enough to create excess vacancies. A considerable amount of vacancies with increasing shear strain was demonstrated by Arkadiusz et al. [16]. The dissociated interstitial H atoms trapped by vacancies is presented in the form called vacancy-hydrogen (Vac-H). Large Vac-H binding energy and high affinity between H atoms and vacancies in some ways lowers the formation energy of a vacancy, which makes it easier for more vacancies to be formed. In addition, the additional vacancies inside the lattice provide easy pathways for dissociated H atoms diffusing into the matrix, which in turn improves the absorption process of the Mg hydrogen storage material [30–36].

##### 4.2. Catalysts

Fine secondary phase particles, acting as catalysts [37,38], which can generally improve the H-kinetics sorption, have already been accepted as a major issue in studies on hydrogen storage properties. Mostly, the fine second phase is supposed to improve the activity for H molecules primarily dissociated/adsorbed on the metal surface as well as for those serving as nucleation sites for the hydride phase, especially for the desorption kinetics.

Soyama et al. [21] investigated the hydrogen storage property of commercial ZK60 magnesium modified with 2.5 wt % mischmetal processed by ECAP and extensive Cold Rolling (CR). The result showed that all the specimens processed by ECAP promoted a significant improvement in hydrogen storage capacity and absorption kinetics. It was the intermetallic particles, which distributed mainly on the grain boundaries during the ECAP processes [37,39], that contributed to the enhancement in hydrogen generation.

Vittori Antisari et al. [40] conducted an experimental research on the nucleation step of the MgH<sub>2</sub> ↔ Mg + H<sub>2</sub> on the basis of metallographic and kinetic data in order to give a clear interpretation of the role of the catalyst particles and the microstructure in the whole process [40]. The results presented a significant increased volume density of nuclei from the pure coarse Mg sample to the ball-milled pure Mg sample, and achieved the maximum density in the Fe-added alloy sample. SEM images indicated that the nucleation site was composed of microstructural defects, mostly distributed along the grain boundaries in pure Mg samples. When Fe was added, a higher density of MgH<sub>2</sub> particles could be found both around the addition elements and in the matrix. This is because the addition elements act as catalyst particles, increasing the nuclei density. The distribution of nuclear sites through the bulk could speed up the reaction.

Montone A et al. [41] later investigated the process of catalyzed Mg reacting with hydrogen to give  $\text{MgH}_2$ . The results suggested that the process of the newly grown  $\text{MgH}_2$  phase was interface-controlled, and the surface of the sample served as the factor limiting the hydrogen flux supplied to the reaction. The limiting factor may be related to the step of splitting the hydrogen molecule on the Mg surface or to the further diffusion through the oxide hydroxide layer which forms on the Mg surface. By adding a catalyst on the surface of the material, it is possible to effectively increase the hydrogen concentration on the surface of the material, thereby accelerating the progress of the reaction [41]. When the reaction rate is increased, the absorption and desorption processes of the catalyzed material can be carried out at lower temperatures compared to the non-catalyzed material [22].

#### 4.3. Grain Boundaries

ECAP can provide UFG metallic materials with a large fraction of high-angle grain boundaries. In fact, the influence of grain boundary on hydrogenation kinetics has been intensively studied. Research showed that hydrogen could diffuse much faster along the grain boundaries [42]. It is important to know the hydrogen behaviors along grain boundaries in order to clarify whether hydrogen is trapped by a grain boundary or passes through the grain boundaries. There are some reports indicating that grain boundaries can serve as easy pathways for hydrogen penetration, which contributes to an improvement in hydrogenation kinetics as well as easy activation [43–45]; others gave the opinion that grain boundaries can act as nucleation sites for the hydride phase [20,40], which also lead to an enhancement in the kinetics of hydrogen absorption and desorption of Mg-based materials.

Kirchheim [46,47] investigated the hydrogen dissolved in nanocrystalline palladium, and his research focused on two regions: along grain boundaries and in the interior region. The results showed that concentrations of hydrogen were mostly distributed on the grain boundaries. Grain boundaries also offered different hydrogen solute site energies which contributed to the enhancement in hydrogen diffusivity along the grain boundary. Recently, Iwaoka et al. investigated the diffusion behavior of hydrogen in SPD-processed UFG palladium by electrochemical permeation tests [48]. The evidence exhibited a more sensitive value of diffusion coefficient with charging current density in SPD-processed metals, both in the absorption step and in the desorption step, compared with that in coarse counterparts. The results also indicated a higher value of diffusion coefficient as well as a lower activation energy in the SPD-processed matrix [48].

It is convincing to suggest that H atoms can enter the interstitial site of the lattice as well as be trapped by defects inside the matrix. When the trap sites are available, H atoms are thought to be more easily chose the lower energy sites along the grain boundaries to be trapped. Actually, the trap effect is much smaller for grain boundaries affecting diffusivity than for vacancies, which is because Except for been trapped, H atoms can also diffuse along the grain boundary. When more H atoms are introduced, H atoms continue to occupy the lower energy sites and begin to pass through higher energy sites where the diffusion activation energy is lower. Calculations have proven that lower activation energy appears along grain boundaries, which means that grain boundaries can function as easy pathways for H atoms to diffuse into the bulk [49–54].

#### 4.4. Textures

In addition to grain refinement and large density of dislocations, ECAP can also introduce changes in metal textures [54].

Jorge et al. [55] investigated the textures produced by ECAP in Mg-based hydrogen storage material. After ECAP processing, the samples were cut into two directions: the cross-sectional plane and the longitudinal plane. The result showed that only the  $\alpha$ -Mg phase existed after ECAP processing. The  $\alpha$ -Mg phase appeared to have preferred orientations in different sections. In the cross-sectional plane, the phase  $\alpha$ -Mg preferred the (101) plane. In the longitudinal plane, the  $\alpha$ -Mg phase was strongly pronounced in the basal (001) plane, and the (001) orientation was the main slip plane for the  $\alpha$ -Mg phase. According to Jorge [55], the (001) orientation is the best orientation for hydrogen absorption.

An (002) crystallographic orientation can be found when ECAP was combined with a subsequent cold rolling process. In the research on pure Mg hydrogen storage material processed by a combination of ECAP and cold rolling, G.F. Lima [56] found that the samples preferred orientation along the (101) direction after four ECAP passes. After cold rolling, the samples acquired were strongly favorable to the (002) orientation. The H-absorption kinetic curves in his research illustrated that samples with a combination of ECAP and CR processing presented a better hydrogen capacity (high up to 5.7 wt %) and a faster hydrogen absorption property than the only ECAP-processed samples (hydrogen capacity is only 2 wt %). Lima thought it was the special texture of the (002) orientation that contributed to the improvement of the hydrogen storage property for samples with processed by both ECAP and CR compared with their only ECAP-processed counterparts.

It has been observed that, the hcp (tetrahedral) and fcc (octahedral) sites are the most possible positions for hydrogen to diffuse into the Mg matrix. Jacobson et al. [57] calculated the binding energies on frozen Mg (001) surfaces, and found that the minimum energy values were for fcc sites at  $-0.88$  eV and for hcp sites at  $-0.852$  eV, and the maximum value was for the Mg atoms sites at  $-0.09$  eV. Weak Phase-Object Approximation Images (WPOA) taken on the three main directions of Mg, (001), (002), and (101), illustrated that, compared with (001) and (101) orientation, (002) texture was much more preferable for hcp (tetrahedral) and fcc (octahedral) sites. In return, these sites could function as stable surfaces for the hydride structure [58]. Moreover, a fixed orientation relationship according to Mg (002)//MgH<sub>2</sub> (110) appeared when the transformation from hydrogenation of the hexagonal Mg structure into rutile MgH<sub>2</sub> occurred [59]. It is reasonable to suggest that the presence of more (002) directions can, to some extent, improve the hydrogen storage property of metal hydrides, because the transformation from Mg to MgH<sub>2</sub> is already favored by the presence of aligned Mg on the correct orientation [57].

## 5. Conclusions and Prospects

The rapid development in nanostructured materials and nanotechnology presents great improvements in surmounting the limitations of bulk Mg-based hydrogen storage materials. Equal Channel Angular Pressing (ECAP) has been proven to be an effective industrial technique in producing bulk ultrafine-grained (UFG) or nanostructured Mg alloys. ECAP also offers many control factors to design the final microstructure. For H<sub>2</sub> storage, the reduced grain size and increased surface area can provide additional binding sites on the surface. Moreover, the large density of vacancies and grain boundaries make it easier for H atoms to diffuse from the surface to the matrix. According to the research performed up to date, the hydrogen storage properties such as the kinetics, capacity, and the cycling stability of UFG Mg are highly promoted by using the ECAP technique. The advantages of UFG Mg hydrogen storage applications have been well introduced, but there still remain many challenges to be settled in the future. The direction of further works could focus on the following points:

1. Mechanism study. The diffusion path for H atoms from the surface to the bulk Mg alloys should be precisely investigated from the atomic scale. Special additives can be added into the bulk to systematically explore the interactions between additive elements and MgH<sub>2</sub>. Advanced theoretical calculations could be used in the research of the MgH<sub>2</sub> hydrogenation/de-hydrogenation process.
2. Microstructure optimization. The present microstructures of UFG or nanostructured Mg alloys need to be optimized on the basis of severe plastic deformation, in order to maximize the positive role for microstructure coordination acting on the hydrogen storage behavior of Mg hydrogen applications, as well as to explore the appropriate microstructures with the maximum hydrogen capacity, kinetic properties, and the longest cycling stability.
3. Electrochemical hydrogen storage property study. Except for the gaseous hydrogen storage condition, UFG Mg alloys are also promising candidates for cathode materials; thus, more attention should be paid to the microstructure control introduced by ECAP to improve the electrochemical hydrogen storage property of UFG Mg alloys by means of microstructure coordination.

**Acknowledgments:** This work was supported by the National Natural Science Foundation of China (Grant No. 51774109), the Key Research and Development Project of Jiangsu Province of China (Grant No. BE2017148), the Fundamental Research Funds for the Central Universities (Grant No. HHU2016B10314), Six Major Talent Peaks Project of Jiangsu Province of China (Grant No. 2014-XCL-023), the Public Service Platform and Science & Technology Support Program in the industrial field of Suqian City of China (Grant No. M201614 & H201615).

**Author Contributions:** This work was carried out in collaboration between all authors. Lisha Wang conducted the literature research, drawn the figures, collected, analyzed, interpreted the data, and finished writing the paper. Jinghua Jiang did the literature research and was responsible for paper revision. Aibin Ma and Dan Song are also responsible for paper revision. Yuhua Li was worked on the literature research. All authors have contributed to the manuscript. The author hopes that this paper can make its due contribution to the successful application and protection of the high-performance ultrafine-grained Mg alloy via ECAP.

**Conflicts of Interest:** The authors declare no conflict of interest.

## References

1. Rusman, N.A.A.; Dahari, M. A review on the current progress of metal hydrides material for solid-state hydrogen storage applications. *Int. J. Hydrogen Energy* **2016**, *41*, 12108–12126. [[CrossRef](#)]
2. International Energy Agency. *World Energy Outlook, Executive Summary*; International Energy Agency: Paris, France, 2010.
3. Skripnyuk, V.M.; Rabkin, E.; Estrin, Y.; Lapovok, R. Improving hydrogen storage properties of magnesium based alloys by equal channel angular pressing. *Int. J. Hydrogen Energy* **2009**, *34*, 6320–6324. [[CrossRef](#)]
4. Wu, D.; Ouyang, L.; Wu, C.; Gu, Q.; Wang, H.; Liu, J.; Zhu, M. A Phase transition and hydrogen storage properties of Mg<sub>17</sub>Ba<sub>2</sub> compound. *J. Alloys Compd.* **2017**, *690*, 519–522. [[CrossRef](#)]
5. Sakintuna, B.; Lamari-Darkrim, F.; Hirscher, M. Metal hydride materials for solid hydrogen storage: A review. *Int. J. Hydrogen Energy* **2007**, *32*, 1121–1140. [[CrossRef](#)]
6. Ellinger, F.H.; Holley, C.E.; McInteer, B.B.; Pavone, D. The preparation and some properties of magnesium hydride. *J. Am. Chem. Soc.* **1955**, *77*, 2647–2648. [[CrossRef](#)]
7. Crivello, J.C.; Denys, R.V.; Dornheim, M.; Felderhoff, M.; Grant, D.M.; Huot, J.; Jensen, T.R.; De Jongh, P.; Latroche, M.; Walker, G.S.; et al. Mg-based compounds for hydrogen and energy storage. *Appl. Phys. A* **2016**, *122*, 85. [[CrossRef](#)]
8. Kim, W.J.; Sa, Y.K. Micro-extrusion of ECAP processed magnesium alloy for production of high strength magnesium micro-gears. *Scr. Mater.* **2006**, *54*, 1391–1395. [[CrossRef](#)]
9. Mostaed, E.; Vedani, M.; Hashempour, M.; Bestetti, M. Influence of ECAP process on mechanical and corrosion properties of pure Mg and ZK60 magnesium alloy for biodegradable stent applications. *Biomatter* **2014**, *4*, e28283. [[CrossRef](#)] [[PubMed](#)]
10. Zeng, K.; Klassen, T.; Oelerich, W.; Bormann, R. Critical assessment and thermodynamic modeling of the Mg–H system. *Int. J. Hydrogen Energy* **1999**, *24*, 989–1004. [[CrossRef](#)]
11. Skripnyuk, V.M.; Rabkin, E.; Estrin, Y.; Lapovok, R. The effect of ball milling and equal channel angular pressing on the hydrogen absorption/desorption properties of Mg–4.95 wt % Zn–0.71 wt % Zr (ZK60) alloy. *Acta Mater.* **2004**, *52*, 405–414. [[CrossRef](#)]
12. Segal, V.M. Materials processing by simple shear. *Mater. Sci. Eng. A* **1995**, *197*, 157–164. [[CrossRef](#)]
13. Valiev, R.Z.; Langdon, T.G. Principles of equal-channel angular pressing as a processing tool for grain refinement. *Prog. Mater. Sci.* **2006**, *51*, 881–981. [[CrossRef](#)]
14. Iwahashi, Y.; Wang, J.; Horita, Z.; Nemoto, M.; Langdon, T.G. Principle of equal-channel angular pressing for the processing of ultra-fine grained materials. *Scr. Mater.* **1996**, *35*, 143–146. [[CrossRef](#)]
15. Huot, J.; Skryabina, N.Y.; Fruchart, D. Application of severe plastic deformation techniques to magnesium for enhanced hydrogen sorption properties. *Metals* **2012**, *2*, 329–343. [[CrossRef](#)]
16. Wiczorek, A.K.; Krystian, M.; Zehetbauer, M.J. SPD processed alloys as efficient vacancy-hydrogen systems. *Solid State Phenom.* **2006**, *114*, 177–182. [[CrossRef](#)]
17. Furukawa, M.; Iwahashi, Y.; Horita, Z.; Nemoto, M.; Langdon, T.G. The shearing characteristics associated with equal-channel angular pressing. *Mater. Sci. Eng. A* **1998**, *257*, 328–332. [[CrossRef](#)]
18. Song, D.; Ma, A.B.; Jiang, J.H.; Lin, P.H.; Yang, D.H.; Fan, J.F. Corrosion behaviour of bulk ultra-fine grained AZ91D magnesium alloy fabricated by equal-channel angular pressing. *Corros. Sci.* **2011**, *53*, 362–373. [[CrossRef](#)]

19. Skripnyuk, V.; Buchman, E.; Rabkin, E.; Estrin, Y.; Popov, M.; Jorgensen, S. The effect of equal channel angular pressing on hydrogen storage properties of a eutectic Mg-Ni alloy. *J. Alloys Compd.* **2007**, *436*, 99–106. [[CrossRef](#)]
20. Asselli, A.A.C.; Leiva, D.R.; Huot, J.; Kawasaki, M.; Langdon, T.G.; Botta, W.J. Effects of equal-channel angular pressing and accumulative roll-bonding on hydrogen storage properties of a commercial ZK60 magnesium alloy. *Int. J. Hydrogen Energy* **2015**, *40*, 16971–16976. [[CrossRef](#)]
21. Soyama, J.; Floriano, R.; Leiva, D.R.; Guo, Y. Severely deformed ZK60 + 2.5% Mn alloy for hydrogen storage produced by two different processing routes. *Int. J. Hydrogen Energy* **2016**, *41*, 11284–11292. [[CrossRef](#)]
22. Crivello, J.C.; Dam, B.; Denys, R.V.; Dornheim, M.; Grant, D.M.; Huot, J.; Jensen, T.R.; De Jongh, P.; Latroche, M.; Milanese, C.; et al. Review of magnesium hydride-based materials: Development and optimisation. *Appl. Phys. A* **2016**, *122*, 97. [[CrossRef](#)]
23. Broom, D.P. The absorption and desorption properties of hydrogen storage material. In *Hydrogen Storage Materials the Characterisation of Their Storage Properties*, 1st ed.; China Machine Press: Beijing, China, 2013. (In Chinese)
24. Krystian, M.; Zehetbauer, M.J.; Kropik, H.; Mingler, B.; Krexner, G. Hydrogen storage properties of bulk nanostructured ZK60 Mg alloy processed by equal channel angular pressing. *J. Alloys Compd.* **2011**, *509*, 449–455. [[CrossRef](#)]
25. Bogdanović, B.; Hartwig, T.H.; Spliethoff, B. The development, testing and optimization of energy storage materials based on the MgH<sub>2</sub>-Mg system. *Int. J. Hydrogen Energy* **1993**, *18*, 575–589. [[CrossRef](#)]
26. Liu, Z.; Lei, Z. Cyclic hydrogen storage properties of Mg milled with nickel nano-powders and MnO<sub>2</sub>. *J. Alloys Compd.* **2007**, *443*, 121–124. [[CrossRef](#)]
27. Lei, Z.; Liu, Z.; Chen, Y. Cyclic hydrogen storage properties of Mg milled with nickel nano-powders and NiO. *J. Alloys Compd.* **2009**, *470*, 470–472. [[CrossRef](#)]
28. Grill, A.; Horkey, J.; Panigrahi, A.; Krexner, G.; Zehetbauer, M. Long-term hydrogen storage in Mg and ZK60 after severe plastic deformation. *Int. J. Hydrogen Energy* **2015**, *40*, 171–178. [[CrossRef](#)]
29. Sato, K.; Yoshiie, T.; Satoh, Y.; Xu, Q.; Kuramoto, E.; Kiritani, M. Point defect production under high internal stress without dislocations in Ni and Cu. *Radiat. Eff. Defects Solids* **2002**, *157*, 171–178. [[CrossRef](#)]
30. Gammer, C.; Karthaler, H.P.; Rentenberger, C. Reordering a deformation disordered intermetallic compound by antiphase boundary movement. *J. Alloys Compd.* **2017**, *713*, 148–155. [[CrossRef](#)]
31. Wang, M.; Vo, N.Q.; Champion, M.; Nguyen, T.D. Forced atomic mixing during severe plastic deformation: Chemical interactions and kinetically driven segregation. *Acta Mater.* **2014**, *66*, 1–11. [[CrossRef](#)]
32. Straumal, B.B.; Mazilkin, A.A.; Baretzky, B. Accelerated diffusion and phase transformations in co-cu alloys driven by the severe plastic deformation. *Mater. Trans.* **2012**, *53*, 63–71. [[CrossRef](#)]
33. Sha, G.; Wang, Y.B.; Liao, X.Z. Influence of equal-channel angular pressing on precipitation in an Al-Zn-Mg-Cu alloy. *Acta Mater.* **2009**, *57*, 3123–3132. [[CrossRef](#)]
34. Ma, A.; Jiang, J.; Saito, N.; Shigematsu, I.; Yuan, Y.; Yang, D.; Nishida, Y. Improving both strength and ductility of a Mg alloy through a large number of ECAP passes. *Mater. Sci. Eng. A* **2009**, *513*, 122–127. [[CrossRef](#)]
35. Setman, D.; Schafler, E.; Korznikova, E.; Zehetbauer, M.J. The presence and nature of vacancy type defects in nanometals detained by severe plastic deformation. *Mater. Sci. Eng. A* **2008**, *493*, 116–122. [[CrossRef](#)]
36. Viswanathan, V.; Laha, T.; Balani, K. Challenges and advances in nanocomposite processing techniques. *Mater. Sci. Eng. R Rep.* **2006**, *54*, 121–285. [[CrossRef](#)]
37. Tran, N.E.; Lambrakos, S.G.; Imam, M.A. Analyses of hydrogen sorption kinetics and thermodynamics of magnesium-misch metal alloys. *J. Alloys Compd.* **2006**, *407*, 240–248. [[CrossRef](#)]
38. Oelerich, W.; Klassen, T.; Bormann, R. Metal oxides as catalysts for improved hydrogen sorption in nanocrystalline Mg-based materials. *J. Alloys Compd.* **2001**, *315*, 237–242. [[CrossRef](#)]
39. Coelho, R.S.; Pinto, H.; Requena, G.C. Casting in the Semi-Solid state of ZK60 magnesium alloy modified with rare earth addition. *Adv. Mater. Res.* **2014**, *922*, 694–699. [[CrossRef](#)]
40. Vittori Antisari, M.; Aurora, A.; Mirabile Gattia, D.; Montone, A. On the nucleation step in the Mg-MgH<sub>2</sub> phase transformation. *Scr. Mater.* **2009**, *61*, 1064–1067. [[CrossRef](#)]
41. Montone, A.; Aurora, A.; Mirabile Gattia, D.; Vittori Antisari, M. On the barriers limiting the reaction kinetics between catalysed Mg and hydrogen. *Scr. Mater.* **2010**, *63*, 456–459. [[CrossRef](#)]

42. Zaluski, L.; Zaluska, A.; Ström-Olsen, J.O. Nanocrystalline metal hydrides. *J. Alloys Compd.* **1997**, *253*, 70–79. [[CrossRef](#)]
43. Hongo, T.; Edalati, K.; Arita, M. Significance of grain boundaries and stacking faults on hydrogen storage properties of Mg<sub>2</sub>Ni intermetallics processed by high-pressure torsion. *Acta Mater.* **2015**, *92*, 46–54. [[CrossRef](#)]
44. Kusadome, Y.; Ikeda, K.; Nakamori, Y.; Orimo, S.; Horita, Z. Hydrogen storage capability of MgNi<sub>2</sub> processed by high pressure torsion. *Scr. Mater.* **2007**, *57*, 751–753. [[CrossRef](#)]
45. Edalati, K.; Yamamoto, A.; Horita, Z.; Ishihara, T. High-pressure torsion of pure magnesium: Evolution of mechanical properties, microstructures and hydrogen storage capacity with equivalent strain. *Scr. Mater.* **2011**, *64*, 880–883. [[CrossRef](#)]
46. Mütschele, T.; Kirchheim, R. Segregation and diffusion of hydrogen in grain boundaries of palladium. *Scr. Mater.* **1987**, *21*, 135–140. [[CrossRef](#)]
47. Mütschele, R.T.; Kirchheim, R. Hydrogen as a probe for the average thickness of a grain boundary. *Scr. Mater.* **1987**, *21*, 1101–1104. [[CrossRef](#)]
48. Iwaoka, H.; Arita, M.; Horita, Z. Hydrogen diffusion in ultrafine-grained palladium: Roles of dislocations and grain boundaries. *Acta Mater.* **2016**, *107*, 168–177. [[CrossRef](#)]
49. Oda, T. Thermodynamic model for grain boundary effects on hydrogen solubility, diffusivity and permeability in poly-crystalline tungsten. *Fusion Eng. Des.* **2016**, *112*, 102–116. [[CrossRef](#)]
50. Hurley, C.; Martin, F.; Marchetti, L.; Chêne, J.; Blanc, C.; Andrieu, E. Role of grain boundaries in the diffusion of hydrogen in nickel base alloy 600: Study coupling thermal desorption mass spectroscopy with numerical simulation. *Int. J. Hydrogen Energy* **2016**, *41*, 17145–17153. [[CrossRef](#)]
51. Wang, F.; Lai, W.; Li, R.; He, B.; Li, S. Fast hydrogen diffusion along the Σ7 grain boundary of α-Al<sub>2</sub>O<sub>3</sub>: A first-principles study. *Int. J. Hydrogen Energy* **2016**, *41*, 22214–22220. [[CrossRef](#)]
52. Sun, L.; Jin, S.; Zhou, H.; Zhang, Y.; Lu, G. Dissolution and diffusion of hydrogen in a molybdenum grain boundary: A first-principles investigation. *Comput. Mater. Sci.* **2015**, *102*, 243–249. [[CrossRef](#)]
53. Oudriss, A.; Creus, J.; Bouhattate, J.; Conforto, E.; Berziou, C.; Savall, C.; Feaugas, X. Grain size and grain-boundary effects on diffusion and trapping of hydrogen in pure nickel. *Acta Mater.* **2012**, *60*, 6814–6828. [[CrossRef](#)]
54. Valiev, R.Z.; Islamgaliev, R.K.; Alexandrov, I.V. Bulk nanostructured materials from severe plastic deformation. *Prog. Mater. Sci.* **2000**, *45*, 103–189. [[CrossRef](#)]
55. Jorge, A.M., Jr.; Prokofiev, E.; Ferreira De Lima, G.; Rauch, E.; Veron, M.; Botta, W.J.; Kawasaki, M.; Langdon, T.G. An investigation of hydrogen storage in a magnesium-based alloy processed by equal-channel angular pressing. *Int. J. Hydrogen Energy* **2013**, *38*, 8306–8312. [[CrossRef](#)]
56. Lima, G.F.; Triques, M.R.M.; Kiminami, C.S.; Botta, W.J.; Jorge, A.M., Jr. Hydrogen storage properties of pure Mg after the combined processes of ECAP and cold-rolling. *J. Alloys Compd.* **2014**, *586*, 405–408. [[CrossRef](#)]
57. Jacobson, N.; Tegner, B.; Schröder, E.; Hyldgaard, P.; Lundqvist, B.I. Hydrogen dynamics in magnesium and graphite. *Comput. Mater. Sci.* **2002**, *24*, 273–277. [[CrossRef](#)]
58. Jorge, A.M., Jr.; Ferreira De Lima, G.; Martins Triques, M.R.; Botta, W.J.; Kiminami, C.S.; Nogueira, R.P.; Yavari, A.R.; Langdon, T.G. Correlation between hydrogen storage properties and textures induced in magnesium through ECAP and cold rolling. *Int. J. Hydrogen Energy* **2014**, *39*, 3810–3821. [[CrossRef](#)]
59. Singh, S.; Eijt, S.W.H.; Zandbergen, M.W.; Legerstee, W.J.; Svetchnikov, V.L. Nanoscale structure and the hydrogenation of Pd-capped magnesium thin films prepared by plasma sputter and pulsed laser deposition. *J. Alloys Compd.* **2007**, *441*, 344–351. [[CrossRef](#)]

